

DOCUMENT CONTROL SHEET

	ORIGINATOR'S REF. NLR-TP-2003-193		SECURITY CLASS. Unclassified				
ORIGINATOR National Aerospace Laboratory NLR, Amsterdam, The Netherlands							
TITLE A Computational Design Engine for multi-disciplinary optimisation with application to a Blended Wing Body configuration							
PRESENTED AT AIAA/ISSMO 2003, Atlanta, USA on 4-6 September 2002							
AUTHORS M. Laban, P. Arendsen, W.F.J.A. Rouwhorst and W.J. Vankan		DATE September 2003	<table border="1" style="width: 100%; border-collapse: collapse;"> <tr> <td style="width: 50%;">PP</td> <td style="width: 50%;">REF</td> </tr> <tr> <td style="text-align: center;">42</td> <td style="text-align: center;">18</td> </tr> </table>	PP	REF	42	18
PP	REF						
42	18						
DESCRIPTORS BLENDED WING BODY MULTI-DISCIPLINARY OPTIMISATION							
ABSTRACT A "Computational Design Engine" for multi-disciplinary design and optimisation of aeronautical products, specially tailored to the needs of a multi-model, multi-level, multi-site environment, is described. The system is illustrated with an application to the Breguet range optimisation of a Blended Wing Body configuration.							



NLR-TP-2003-193

A Computational Design Engine for multi-disciplinary optimisation with application to a Blended Wing Body configuration

M. Laban, P. Arendsen, W.F.J.A. Rouwhorst and W.J. Vankan

This report is based on a presentation held at AIAA/ISSMO 2003, Atlanta, USA, 4-6 September 2002.

The contents of this report may be cited on condition that full credit is given to NLR and the authors.

Customer: National Aerospace Laboratory NLR
Working Plan number: A.1.B.5, S.3.A.3, V.1.A.3, I.1.A.5
Owner: National Aerospace Laboratory NLR
Division: Aerodynamics, Structures, Flight Mechanics, Informatics
Distribution: Unlimited
Classification title: Unclassified
September 2003

Approved by author: <i>ML 17/9</i>	Approved by project manager: <i>Ⓢ 17/9/2003</i>	Approved by project managing department: <i>BO 18/9'03</i>
---------------------------------------	--	---



Summary

A "Computational Design Engine" for multi-disciplinary design and optimisation of aeronautical products, specially tailored to the needs of a multi-model, multi-level, multi-site environment, is described. The system is illustrated with an application to the Breguet range optimisation of a Blended Wing Body configuration.



Contents

1	Introduction	7
2	Optimisation Strategy	9
3	The Computational Design Engine	10
3.1	Geometry Generation	10
3.2	Weight and Balance	11
3.3	Structural Optimisation	11
3.4	Aerodynamic Cruise Performance	14
3.5	Flight Mechanics	15
3.6	Objectives and Constraints	17
4	Application to Blended Wing Body Optimisation	19
5	Conclusions and Outlook to the Future	22
5.1	Acknowledgements	22
6	References	23

18 Figures

(42 pages in total)



Nomenclature

Abbreviations

ASCII	American Standard Code for Information Interchange
BWB	Blended Wing Body
CAP	Control Anticipation Parameter
CDE	Computational Design Engine
CM	Controllability Margin
FAA	Federal Aviation Administration
FAR	Federal Aviation Regulations
FEM	Finite Element Model
FCS	Flight Control System
IGES	Initial Graphics Exchange Specification
HQ	Handling Qualities
JAR	Joint Aviation Regulations
MDO	Multi-Disciplinary Optimisation
MOB	Project acronym for Brite-Euram project: A Computational Design Engine Incorporating Multi-Disciplinary Design and Optimisation for Blended Wing Body Configuration
MTOW	Maximum Take-Off Weight
OEW	Operating Empty Weight
PCL	Patran Command Language
TFW	Trip Fuel Weight
T2	Time to double
2D	Two-Dimensional
3D	Three-Dimensional



Symbols

C_D	Drag coefficient
C_L	Lift coefficient
C_m	Pitching moment coefficient
c	Chord
D	Drag
G	Acceleration due to gravity
g	Flutter damping coefficient, acceleration due to gravity
H	Specific heat of combustion
L	Lift
M	Mach number
q	Pitch rate
R	Range
T	Thickness
V	Velocity
V_{min}	Minimum speed
V_r	Rotation speed
W	Weight
x_{cg}	X-coordinate centre of gravity
x_{np}	X-coordinate neutral point
z	Z-coordinate wing profile
α	Angle-of-attack
δ	Control surface deflection angle
δ_e	Elevon deflection angle
δ_a	Symmetric aileron deflection angle
δ_T	Engine exhaust nozzle deflection angle
η	Engine fuel efficiency
θ	Design variable
σ	Stress

1 Introduction

A *Computational Design Engine*, or shortly CDE, for design and optimisation of aeronautical products tailored to the needs of a *multi-disciplinary, multi-model, multi-level, multi-site*, environment is described. The CDE integrates a range of individual discipline based tools with "Multi-disciplinary Design and Optimisation" (MDO) methodologies. It ensures continuity of information flow through the design stages from concept to, in principle, main phase design using appropriate levels of fidelity of physical models (multi-model). Additionally, different levels of scope and detail are used (multi-level). The design process being modeled reflects the situation in Europe, i.e. parts of the design are made concurrently by different companies at physically different locations (multi-site).

The CDE is demonstrated by application to a design problem of intrinsic interest, namely a Blended Wing Body (BWB) aircraft. This configuration is studied as a potential successor to large conventional aircraft, offering room to further reduction of the environmental impact of aviation (Ref. 1). Future realisation of this large transport aircraft concept, with inherent strong coupling between disciplines, calls for innovative methodologies to reduce non-recurrent cost of design and development. This aspect makes the Blended Wing Body aircraft ideally suited to study the Computational Design Engine for multi-disciplinary optimisation.

The CDE, as configured to the optimisation of the BWB configuration, involves three main disciplines: Aerodynamics, Structural Mechanics and Flight Mechanics. The multi-model nature of the design process implies that different sets of analysis tools are used, applicable to the level of maturity of the product at each stage. For the Aerodynamics discipline, the tools used range from panel codes, Euler codes, to full Navier-Stokes analyses taking trim and aeroelastic deformations into account. For the Structural Mechanics discipline, the tools used range from engineering "Bending Beam Theory" to full blown Finite Element Model (FEM) based structural optimisation including aeroelastic constraints. For the Flight Mechanics discipline the tools range from a low-fidelity stability and controllability analysis to a full handling qualities analysis of the closed-loop aircraft system. To expedite convergence of the iterative schemes within the CDE, only the essential strong couplings between disciplines are taken into account. Thus the strong coupling between Structural Mechanics (structural weight, flexible deformations) and Aerodynamics and its effect on flight characteristics are modeled. Additionally, the coupling between centre of mass and the centre of aerodynamic force ("trim"), which is crucial to a tailless aircraft concept, is taken into account in all disciplines.



Results are shown for the CDE system being applied to the Breguet range optimisation of the BWB configuration under assumption of constant Maximum Take-Off Weight (MTOW). Both the aerodynamics discipline (lift over drag ratio in transonic cruise) as well as the structural mechanics discipline (structural weight) contribute directly to the overall design objective. The Flight Mechanics discipline brings constraints on the centre of gravity margin to intolerable flight characteristics.

2 Optimisation Strategy

The optimisation strategy is based on a multi-level approach with a multi-disciplinary aircraft design task on the global level and a structural design task on the local level. The global level comprises only those design parameters which impact all disciplines; typically a limited set of (e.g. planform) parameters. On a local structural level several hundred groups of FEM-element thicknesses are used as design variables.

For the global level design task a *Response Surface* (Ref. 2) strategy is preferred over gradient based optimisation schemes. Reasons for this are threefold. First, most analysis modules do not have sensitivity analysis capabilities which is required for efficient gradient based optimisation. Secondly, the opportunity to relax the timing of the various tasks over the multiple sites, partners and disciplines. This opens ways to efficient parallel processing. At last, the number of global design variables is small, making scanning the design area affordable. A response surface represents the shape of the objective and constraint functions in the design space and thereby provides excellent means to visualize the trade-offs between the various disciplines.

Inside the local structural design task the situation is different. Sensitivity information is available. Moreover, the number of design variables is such that gradient based optimisation is more effective.

A response surface methodology requires evaluation of properties of aircraft variants at a priori selected points in the design space, Ref. 2. This information is provided by the *Computational Design Engine*, Figure 1.



3 The Computational Design Engine

Figure 2 introduces the main functional modules of the CDE. These comprise:

- A *Geometry* module providing internal (structural) and external (aerodynamic) shapes of the configuration.
- A *Weight and Balance* module keeping a record of all items contributing to the weight of the configuration.
- A *Structural Optimisation* module computing a minimum weight internal aircraft structure.
- An *Aerodynamic Performance* module analysing the aircraft lift over drag (L/D) performance under transonic cruise conditions.
- A *Flight Mechanics* module assessing the stability, controllability, and handling qualities of the configuration.
- An *Objective and Constraints* module which collects the results from all contributing analysis disciplines and computes the values of the global-level design objective and constraints.

The CDE itself consists of a collection of UNIX shell scripts and executable programs made available by the contributing partners. In order to link all these scripts and all the computers on different networks across Europe, the middleware system SPINeware (Ref. 3) is used. Additionally SPINeware serves as a graphical user interface enabling the designer to use the CDE and concentrate on the design problem instead of hardware and software issues.

The following sections provide information on the individual CDE modules and show analysis results of the Cranfield University designed Blended Wing Body (BWB) reference aircraft which serves as point of departure for the subsequent optimisation process (Chapter 4).

3.1 Geometry Generation

The *Geometry Module* is responsible for defining the internal (structural) and external (aerodynamic) shape of the configuration as well as the location of the aircraft systems. It accepts parametric inputs (i.e. values for wing sweep, wing area, wing aspect ratio etc.) through which it interfaces to the *Experiment Setup* module of Figure 1.

Geometry modeling for the Blended Wing Body configuration is performed by the University of Delft using ICAD, Ref. 4. The data describing the external shape is delivered as a set of points. The internal structure is delivered as IGES files. Information on the location and mass of the aircraft systems is provided in an ASCII table.

3.2 Weight and Balance

The *Weight and Balance* module is responsible for keeping a record of all items contributing to the weight of the aircraft. The flight mechanics and aerodynamics disciplines require additional knowledge in terms of centre of gravity location and moments of inertia. Items are classified according to:

- *Nonstructural Items* comprise items not belonging to the primary aircraft structure (e.g. systems). Saab provided a methodology based on conceptual design methods to estimate the weight of the various components (for most items, this is simply a fraction of MTOW). The total nonstructural mass for the BWB reference configuration is $W_{nonstructural} = 65158$ kg. Figure 3 illustrates the location of the various nonstructural items relative to the external shape of the configuration.
- *Structural Items* comprise items like ribs, beams, stiffeners, skin panels, etc. This information is obtained from the Structural optimisation module (Section 3.3). The total structural mass for the BWB reference configuration is $W_{structural} = 57243$ kg, Operational Empty Weight (OEW) is $W_{OEW} = 122401$ kg.
- *Payload* comprise LD3 containers (freighter configuration). For the BWB configuration, a fixed 113 tons of payload is carried in 174 LD3 containers distributed over a double deck cargo hold. The distribution of the containers over the cargo hold is provided by Cranfield University, see Figure 4.
- *Fuel* stored in two body trim tanks and in the main wing tanks. A fuel scheduler controls the filling and draining of tanks to ensure control over the aircraft centre of gravity. The distribution of fuel is different for each individual loadcase driving the various disciplines, Figure 5 shows an example. Available trip fuel weight (TFW) is computed as the difference between MTOW and the sum of nonstructural weight, structural weight, and payload weight. For the BWB configuration, MTOW is fixed at $W_{MTOW} = 371280$ kg, hence trip fuel weight for the reference configuration is $W_{TFW} = 135878$ kg.

The *Weight and Balance* module is assigned the task to assemble the individual mass components into critical loadcases. For each loadcase, a full set of information comprising mass, centre of gravity, moments of inertia, flight condition etc. is generated and written to the CDE database. This data presents the driving scenario for the subsequent analysis disciplines for assessment of aerodynamic cruise performance, structural weight, and aircraft controllability.

3.3 Structural Optimisation

The *Structural Optimisation* module is responsible for sizing the primary structural elements of the configuration such that it can withstand all loads that may occur during the lifetime of the aircraft. The driving scenario is currently limited to a single load case: i.e. a +2.5G pull-up manoeuvre

at sea-level altitude and Mach=0.50. The aircraft payload/fuel loading is configured such that the (wing) structure experiences maximum bending moments with minimal inertial relief: i.e. maximum payload, full body trim tanks, and empty wing tanks.

Figure 6 shows how the structural optimisation is embedded in a loop interacting with an aerodynamic loads evaluation module. The aerodynamic loads are extracted from the surface pressure distribution and mapped onto the structural model. An iterative scheme arises as the, a priori unknown, structural mass distribution is fed back to the aerodynamics module through "weight and balance". Modeling a flexible aircraft through incorporating stiffness feedback from the structural optimisation to the aerodynamic load generator in this loop is "work in progress".

The aerodynamic loads are generated using the NLR ENFLOW system. This multi-block flow solver is operated in Euler mode and features aeroelastic coupling and trim. During the flow solver iterations the angle-of-attack and trailing edge control surface deflections are updated to arrive at the prescribed lift (2.5 times the aircraft mass) and pitching moment trim (centre of aerodynamic force coinciding with centre of mass). This trimming loop is essential as the deflections of the trailing edge control devices alter the spanloading and hence the wing bending moments. Section 3.4 provides more details on the aerodynamics discipline.

A minimum weight structural optimisation is carried out with stress and aeroelastic (flutter) constraints. Methods with different levels of fidelity (multi-model) are implemented in the CDE,

- Low-fidelity: Bending beam theory.
- High-fidelity: Finite Element Modeling.

In bending beam theory, the forces required for equilibrium between the aerodynamic loads and the inertial loads run through the configuration skin. The analysis proceeds by reducing all loads information to spanwise bending and torsion moments. Contributors to inertial loads are: the non-structural items, the structural elements, payload, and fuel. Skin thickness is chord-wise constant but varies in span direction. Spanwise thickness is minimised such that the peak Von Mises stress reach the upper allowable level of 250 N/mm^2 at each span station.

The high fidelity structural module is based on the finite element method implemented in NAS-TRAN. The optimisation objective is minimum weight. The optimisation constraints are element thickness $T > 2 \text{ mm}$, Von Mises stress level $< 250 \text{ N/mm}^2$, flutter damping $g > 0.03$ at $V = 300 \text{ m/s}$ and sea-level altitude. Element thickness, grouped in so called design areas, are used as design variables.

The layout of the aircraft structure, including identification of surfaces, materials and design areas, is provided by the geometry module using ICAD. BAe-Systems defined a PCL script driven

PATRAN session file, Ref. 5. This script reads the ICAD data, meshes the topology and applies loads and boundary conditions. An additional program MAPSURF is used to map design areas and surfaces from ICAD to PATRAN, including design information such as: material type, stress allowable, initial values, etc. These combined script and programs then fully automatically generate the NASTRAN bulk data deck file necessary to run the optimisation. The transfer of aerodynamic surface pressures onto the structural mesh is done using a BAe-Systems developed program named PALMS, Ref. 6. As a result a set of loadcards is generated which are included in the NASTRAN analysis.

The flutter constraint is based on the NASTRAN SOL144/SOL200 solution. The aerodynamics used for this solution is a linear Doublet Lattice technique. DLR provides a Transonic Doublet Lattice method in combination with ZAERO (Ref. 7), for improved quality of the results at transonic speeds (Ref. 8). This capability will be linked to the CDE later in the project.

Figure 7 shows the distribution of 227 design variable areas of the Blended Wing Body reference aircraft. Figure 8 shows the NASTRAN weight optimised, thickness/stress/stiffness constrained element thicknesses.

The primary aircraft structure, shown in Figure 7, does not include structural details like: doors, windows, control surface supports, engine attachments, etc. Additionally, manufacturing constraints are not taken into account, such as discrete material thicknesses and joints. In preliminary design, statistical methods are used to estimate these mass contributions. Several studies address this problem, Ref. 9, 10, 11, and suggest the use of a scale factor of 1.5 between the FEM-based structural mass and the real-live aircraft structural mass. The inclusion of detail structural design is a way to decrease this (uncertain) compensation factor. Future work within the project incorporates a structural multi-level capability to design major structural details like doors on a local level. This activity is pursued by the University of Siegen. This multi-level design approach also ensures continuity of information flow from structural main phase design to the structural detail design phase.

The final outputs from the structural optimisation module are: structural weight, centre of gravity, and moments of inertia. These are computed from the optimised element thicknesses (including the scale factor of 1.5) and supplied to the CDE database. The resulting structural mass for the Blended Wing Body reference aircraft based on bending beam theory is: $W_{structural} = 57243$ kg, $x_{cg_{structural}} = 31.21$ m and the results based on FEM analysis is: $W_{structural} = 66521$ kg, $x_{cg_{structural}} = 34.00$ m.



3.4 Aerodynamic Cruise Performance

The global-level optimisation objective, Breguet Range, calls for an evaluation of the configuration lift over drag (L/D) performance during transonic cruise (Section 3.6). The driving scenario is a mid-cruise flight condition at Mach=0.85, 35000 feet altitude in standard atmosphere conditions, maximum payload on board, half the trip fuel available in the wing tanks and empty body trim tanks. Tailless aircraft longitudinal trim, by means of deflecting partial-span trailing edge devices, does have a serious impact on the aerodynamic efficiency in cruise and needs to be accounted for in the analysis.

The most efficient prediction of aerodynamic drag is obtained using Navier-Stokes flow solvers operating on *block-structured* grids. The NLR ENFLOW system is used to provide this information for the BWB configuration. This system supports aeroelastic deformation (static and dynamic) and features a capability to incorporate pitching moment trim by means of mode shapes, Ref. 12. Moreover, the ENFLOW system can be setup to operate fully autonomously without manual user interaction.

The first task to be performed is domain decomposition using the ENDOMO utility. This is initiated manually by decomposing the BWB reference aircraft surface into various domains. Using an electrostatic analogy, Ref. 13, the 3D spatial block-boundaries for the BWB reference aircraft are automatically grown into 3D space. The resulting block-topology is mapped to all subsequent design variants using volume spline techniques, Ref. 14. Figure 9 provides an example.

The second task is multi-block grid generation using the ENGRID utility. ENGRID requires the user to specify the non-dimensional grid densities and grid stretchings along all block edges. This process is fully parametric, and once set up manually, can be applied in a robust and automated way to all aircraft variants. Figure 10 shows an example of the Navier-Stokes grid on the configuration surface and symmetry plane.

The third task is the definition of the *mode shapes* representing the trailing edge control surfaces which will be employed to trim the aircraft. Volume spline techniques are used to incorporate the control surface deflections into the configuration surface and 3D volume grid.

Finally the flow solver utility ENSOLV is run in Navier-Stokes mode using the $k - \omega$ turbulence model, Ref. 15. The flow solver is iterated until the target lift coefficient C_L is reached and the pitching moment coefficient C_m around the centre of gravity converges to zero. This is done by a loop that feeds back the aerodynamic forces to the angle-of-attack α and mode shape amplitudes δ during the flow solver iterations. The loop feedback gains are optimised with a priori estimates of

the aerodynamic derivatives $C_{L\alpha}$, $C_{m\alpha}$, $C_{L\delta}$, $C_{m\delta}$ under transonic conditions. The resulting drag coefficient is extracted from the surface pressure and friction distributions and lift over drag ratio (L/D) is returned to the CDE database.

Figure 11 shows an example of the resulting surface pressure distribution for the BWB reference aircraft. The lift over drag ratio is $L/D = 16.82$.

3.5 Flight Mechanics

The flight mechanics module is responsible for the assessment of the longitudinal (in)stability and controllability of the BWB aircraft for all weight and centre of gravity (x_{cg}) combinations that can occur (JAR/FAR/FAA certification requirement). As the most critical condition occurs at low dynamic pressure, a low-speed approach flight scenario drives the flight mechanics assessment. This evaluation comprises open-loop as well as closed-loop analysis.

The Weight and Balance discipline provides the mass distribution of the various aircraft components. This information is used to build up an aircraft *weight and balance envelope*, Figure 12, which shows the situation for the two limiting cases of zero-payload (in blue) and full-payload (in green). For the full-payload case, the wing tanks are used exclusively. For the zero-payload case, weights up to OEW + TFW are considered. In that case, the forward body trim tank (50 tons capacity) is used first, after which fuel carries over to the main wing tanks. Figure 12 shows how the aircraft *actual* centre of gravity is assessed versus the aircraft *tolerable* centre of gravity boundaries (in black) dictated by the flight mechanics constraints (discussed below).

Computing the *tolerable* centre of gravity range calls for information on the aerodynamic forces and moments for departures from equilibrium flight at low-subsonic speeds. This information is provided using panel methods by NLR (PDAERO) or Cranfield University (WINGBODY). The results are expressed as linear expansions of the non-dimensional lift coefficient (C_L) and pitching moment coefficient (C_m). E.g. for the BWB reference aircraft these read ($x_{cg} = 33.22m$):

$$C_L = -0.401 + 5.76 \cdot \alpha + 2.22 \cdot \delta_e + 0.74 \cdot \delta_a \quad (1)$$

$$C_m = -0.001 + 0.77 \cdot \alpha - 0.71 \cdot \delta_e - 0.45 \cdot \delta_a \quad (2)$$

in which δ_e indicate the inboard trailing edge control surface deflections (elevons) and δ_a indicate symmetric deflections of the outboard trailing edge controls (ailerons). Downward deflection angles are positive. Panel methods allow to compute the aerodynamic angle-of-attack derivatives ($C_{L\alpha}$, $C_{m\alpha}$) efficiently once the matrix of influence coefficients has been computed. Finite differencing is applied to find the control surface derivatives. Furthermore, the angle-of-attack at

maximum lift is required. This is derived from a time-accurate Navier-Stokes solution for the configuration with deployed leading edge slats during a dynamic stall manoeuvre, see Figure 13. Due to the high computational effort, this computation is done only once for the BWB reference aircraft and the resulting effective angle-of-attack ($\alpha = 27^\circ$) is used for all subsequent design variants.

With the available aerodynamic data, the flight mechanics discipline computes the neutral point (x_{np}) and the *tolerable* forward as well as rearward centre-of-gravity (x_{cg}) boundaries according to five longitudinal assessment criteria (Figure 12 illustrates these boundaries for the BWB reference aircraft). The first criterion applies to the take-off ground run for which a rotation speed $V_r = 140$ knots is taken as representative for a heavy-weight transport aircraft. The remaining criteria apply to an approach flight phase at 140 knots. Adopting the required 30 percent speed safety margin on approach, this implies that the aircraft must be operated safely down to $V_{min} = 110$ knots airspeed. It is assumed that a full-authority flight control system (FCS) will not permit airspeeds below 110 knots, such that the certification requirement of demonstrating controllable handling up to the actual stall speed need not be demonstrated in the usual way. The five assessment criteria are:

- Take-off rotation control power at V_r

A limit on the forward centre of gravity location is obtained from the constraint that the aircraft must be able to generate sufficient pitch up acceleration ($\dot{q} = +3/s^2$) for rotation during an accelerated take-off ground run, Ref. 16. The conditions at rotation are: $V = 70m/s$, $\alpha = +10^\circ$, $\delta_e = -20^\circ$, $\delta_a = -10^\circ$, $\delta_T = -20^\circ$ (engine exhaust nozzle deflection angle).

- Maximum elevon deflection boundary at V_{min}

A limit on both the forward and rearward centre of gravity location is obtained from the constraint that the elevon trim angles of the aircraft do not exceed the maximum values of $+/- 20^\circ$. The conditions are: $V = 55m/s$, α as required for lift to meet aircraft weight for a 1G flight, $\delta_a = 0^\circ$.

- Maximum angle-of-attack boundary at V_{min}

A limit on the forward centre of gravity location is obtained from the constraint that the angle of attack of the (elevon-) trimmed aircraft does not exceed the angle-of-attack at stall. The conditions are: $V = 55m/s$, $\alpha = +27^\circ$, δ_e as required for pitching moment trim, $\delta_a = 0^\circ$.

- 1G push-over control power at V_{min}

A limit on the rearward centre of gravity location is obtained from the constraint that the aircraft must have sufficient push-over capability ($\dot{q} = -5.5/s^2$) at minimum speed, Ref. 17.

The conditions are: $V = 55\text{m/s}$, α as required for lift to meet aircraft weight for a 1G flight, $\delta_e = +20^\circ$, $\delta_a = +10^\circ$.

- Time-to-double (T2) criterion at V_{min}

For unstable aircraft ($x_{cg} > x_{np}$) controllability should be assured by the FCS (the BWB reference aircraft is unstable for low weights near OEW). However, a limit on the rearward centre of gravity location is obtained from the constraint that the time-to-double of flight path distortions must remain limited to allow any divergent motion to be counteracted within sufficient time, Ref. 18. T2 relates to C_{m_α} via the actual x_{cg} location. The minimum value is set at $T2 = 0.8\text{s}$. The conditions are: $V = 55\text{m/s}$, $\delta_e = +20^\circ$, $\|\dot{\delta}_e\| = 20^\circ/\text{s}$, $\delta_a = 0^\circ$.

Figure 12 illustrates the overall constraint, the *Controllability Margin* (CM). The controllability margin quantifies the most critical distance along the x_{cg} -axis between the *tolerable* and the *actual* W - x_{cg} envelopes. A positive CM value indicates that favorable conditions prevail for sufficient longitudinal controllability. A negative value indicates that a constraint is violated.

Following the open-loop static stability analysis, the longitudinal handling qualities (HQ) of the BWB aircraft plus preliminary flight control system (FCS) are assessed for an approach flight condition at $V=70\text{ m/s}$, sea-level altitude, and aft centre of gravity at OEW, Ref. 8. The longitudinal HQ criteria applied are: Bandwidth, Control Anticipation Parameter (CAP), Rise time, Transient peak, Time delay, Dropback and C-star. An automated Linear Quadratic Regulator based design method derives the gains for full state-feedback. Other FCS element parameters (e.g. stick and actuator servo dynamics) inside the predefined longitudinal control law structure remain fixed. The assessment results into the assignment of a HQ level 1, 2 or 3 per criterion. The BWB reference configuration features HQ level 2 for CAP and Time delay, and HQ level 1 for the other criteria.

The definition and implementation of appropriate lateral handling constraints for a Blended Wing Body aircraft is on-going. The driving scenario will include take-off engine failure and cross-wind landings. Preliminary analysis performed by Cranfield University revealed directional static instability at high angle-of-attack and rearward centre of gravity position.

3.6 Objectives and Constraints

Possible choices for the global-level optimisation objective are:

- Direct Operating Cost
- Breguet Range

The Direct Operating Cost option is probably the "ultimate" choice in which the cost is computed for a specified mission (i.e. to carry a fixed payload over a fixed range). Unfortunately, the associated cost function is driven by economical considerations/predictions and is not easily accessible.

Effect of structural weight savings, or aerodynamic drag reductions, generally give rise to a waterfall reaction, e.g. one kilo of structural weight saving, or 1 count of drag saving, gives rise to a reduction of e.g. engine and gear size and thus weight. This in turn gives rise to jet another cycle of structural weight savings and further drag reductions. Multiple expensive analysis loops will be required for each candidate aircraft design before this process converges.

A more realistic option is to use range at a fixed Maximum Take Off Weight (MTOW) as the objective function. The concept of fixed-MTOW effectively breaks the aforementioned "waterfall" loop as all nonstructural items will more or less keep their fixed weights as well. One kilogram of structural weight saving is now returned as one additional kilogram of fuel weight,

$$W_{fuel} = (W_{MTOW} - W_{payload} - W_{nonstructural}) - W_{structural} \quad (3)$$

The global-level objective function chosen in the Blended Wing Body optimisation study is *Breguet Range* (R):

$$R = \left(\eta \frac{H}{g}\right) \cdot \left(\frac{L}{D}\right)_{cruise} \cdot \ln\left(\frac{W_{MTOW}}{W_{MTOW} - W_{fuel}}\right) \quad (4)$$

which is representative for (though not equal to) the true operational aircraft range. The direct contribution of the aerodynamics discipline to range is straightforward through the term $\left(\frac{L}{D}\right)_{cruise}$. The contribution of the structural mechanics discipline is less direct as it runs through the available fuel mass. Note that the relation between structural mass savings and range is non-linear in the Breguet equation.

Assuming an engine efficiency of $\eta = 0.34$ and a kerosine specific heat of combustion $H = 43.4 \text{ MJ/kg}$, the Breguet range for the BWB reference aircraft is equal to $R = 11263 \text{ km}$.

The global-level optimisation constraint is the *Controllability Margin* (CM) as delivered by the flight mechanics module. The value of this constraint must remain positive to ensure controllable flight (c.f. Section 3.5). For the BWB reference aircraft the Controllability Margin is equal to $CM = -977 \text{ mm}$. Hence, the reference configuration does not feature sufficient controllability. This observation sets the stage for an optimisation run applying the CDE to the Blended Wing Body Configuration to remedy this situation.

4 Application to Blended Wing Body Optimisation

The CDE is demonstrated using the Blended Wing Body concept as the driving scenario. The design task is to restore controllability while, at the same time, the Breguet range is to be maximised. On the global level, 5 design parameters are released for optimisation; i.e. θ_1 = wing-twist, θ_2 = wing-thickness, θ_3 = wing-sweep, θ_4 = fuselage-length, and θ_5 = fuselage-camber. On a local level, low-fidelity structural mechanics is used.

The individual effects of the selected design parameters are surveyed during a first optimisation run in which the design parameter values are changed one-by-one, keeping the other design variables fixed at the values inherited from the BWB reference configuration (1D optimisation). For this purpose second order polynomial expansions are used to build up the response surfaces:

$$y(\theta_i) = C_1 + C_2 \cdot \theta_i + C_3 \cdot \theta_i^2 \quad , \quad i = 1..5 \quad (5)$$

in which θ_i represents the value of the i-th design parameter and $y(\theta_i)$ represents the response of either the value of the objective or the value of the constraint function as a result of a change in the value of the i-th design parameter. The polynomial coefficients C_1 , C_2 and C_3 attain different values for each 1D optimisation study and are determined using a Least Squares fitting procedure applied to the available aircraft variant dataset. When this dataset comprises at least three entries, i.e. three different choices for the value of θ_i , the individual polynomial coefficients become identifiable. As data for the reference aircraft is already available, this calls for the analysis of two additional aircraft variants per design variable.

Aircraft variants are generated through design parameter offsets, $\Delta\theta_i$, from their nominal values, θ_i^{ref} , inherited from the BWB reference configuration. The parameter offset definitions are:

- 3° wing-twist offset, applied with zero twist at the root and increasing linearly with span to the full value at the wing tip ($\Delta\theta_1 = 3$),
- 10 percent relative wing thickness offset, applied to all wing profiles
($z/c = \theta_2 * z^{ref}/c$, $\theta_2^{ref} = 1.00$, $\Delta\theta_2 = 0.10$),
- 3° wing-sweep offset ($\Delta\theta_3 = 3$),
- 3 m fuselage-length offset ($\Delta\theta_4 = 3$),
- 1 per cent fuselage aft-camber offset, applied to all fuselage profiles
($z/c := z^{ref}/c - \theta_5/100 * \sin(2\pi(x/c)^2)$, $\theta_5^{ref} = 0$, $\Delta\theta_5 = 1$).

All offsets are applied with negative ($\theta_i = \theta_i^{ref} - \Delta\theta_i$) and with positive ($\theta_i = \theta_i^{ref} + \Delta\theta_i$) sign. This gives rise to 10 aircraft variants which were analysed by the CDE using a cluster of 4 Silicon Graphics workstations each running upto 3 aircraft variants overnight.

The 1D optimisation results already provide useful information to the designer. For example, it provides a feeling for the relative effects of the individual parameters on the objective and constraint values and allows to fine-tune the step size of the design parameter offsets, $\Delta\theta$. Although almost all individual parameters are found to effect controllability, no single parameter was found that could restore the aircraft controllability margin (CM) to positive values.

The design task continues with a second optimisation run in which the effect of all combinations of two design parameters, θ_i and θ_j , are explored (2D design subspaces). For this purpose, second order polynomial expansions are used to build up the response surfaces:

$$y(\theta_i, \theta_j) = C_1 + C_2 \cdot \theta_i + C_3 \cdot \theta_j + C_4 \cdot \theta_i^2 + C_5 \cdot \theta_i\theta_j + C_6 \cdot \theta_j^2 \quad (6)$$

in which θ_i and θ_j represent the values of the combinations of i-th and j-th design parameters and $y(\theta_i, \theta_j)$ represents the reponse of the objective or constraint function. A *full-factorial* (Ref. 2) aircraft variant data set is build up consisting of all possible combinations of the parameter values $\theta_i^{ref} - \Delta\theta_i, \theta_i^{ref}, \theta_i^{ref} + \Delta\theta_i$ with $\theta_j^{ref} - \Delta\theta_j, \theta_j^{ref}, \theta_j^{ref} + \Delta\theta_j$. This results in 9 data sets per 2D design sub-space, for which the 6 unknown polynomial coefficients C_1 through C_6 are determined using Least Squares techniques.

Re-using the data sets already available from the 1D design space explorations, this gives rise to 40 additional aircraft variants (indicated as aircraft variant numbers 12 through 51) which were analysed by the CDE again using a cluster of Silicon Graphics workstations running over a weekend.

From the resulting 2D combinations of design parameters, the designer starts building up knowledge on which combinations of design variables are most effective in reaching the design targets. For example, from all 10 2D design subspace combinations available, the combination of fuselage-camber versus wing-sweep and fuselage-camber versus fuselage-length (Figure 14) are both equally effective in driving the design closer towards the feasible design space. Figure 15 shows the impact on the overall design objective (Breguet range). Figure 15 also illustrates the trade-offs between the structural weight changes and aerodynamic cruise L/D efficiency changes.

The conclusion from the 2D optimisation study is that controllability can be improved by shortening the fuselage and increasing the aft-camber of the fuselage profiles. The impact on the overall design objective (Breguet range) will be negative.

The data set of 51 aircraft variants allows to inspect all 10 3D design subspace combinations as well, although it is then no longer a *full factorial* approach. From a visual inspection of the

response surfaces, the wing-twist, fuselage-camber, and fuselage-length combination seems most promising. One additional design entry was processed by the CDE to get one additional point supporting the 3D response surface near the expected optimum in the design space. Figures 16 and 17 present the results. The response surface predicts that the -3° twisted wing, 3 m shortened fuselage and "1 per cent aft-cambered" fuselage profiles (i.e. $z/c = z^{ef}/c - 0.01 * \sin(2\pi(x/c)^2)$) restores full controllability. This is confirmed by Figure 18 which is the CDE analysis result for this particular design variant ($CM = +8 mm$). The closed-loop aircraft HQ levels of this design variant are equal to those of the reference aircraft. The price to be paid for restoring controllability in this 3D design subspace is high. Breguet range went down from $R = 11263 km$ for the insufficiently-controllable BWB reference aircraft to $R = 9918 km$ for the controllable design variant.

Optimal Design of Experiments (Ref. 2) techniques are employed in the exploration of the 4D and 5D design subspaces where the full-factorial approach does become prohibitively expensive. This work is in progress.



5 Conclusions and Outlook to the Future

A *Computational Design Engine*, or CDE, for multi-disciplinary design and optimisation specially tailored to the needs of a multi-model, multi-level, multi-site environment is designed and implemented. The objective of the CDE is to ensure continuity of information flow through the design stages from concept to main phase design using appropriate levels of fidelity of physical models. This is seen as an important contribution to minimise the non-recurring product development costs.

The system is demonstrated with an application to a Blended Wing Body configuration. The optimisation of this concept poses an interesting challenge due to the strong coupling of the various disciplines, which is inherent to a tailless concept. In early stages of aircraft design optimisation, the CDE was used to explore the various design subspaces which are most effective to bring the design into the feasible region. This is then followed by a more performance driven optimisation stage whereby more and more design variables are introduced.

In the near future, new analysis modules will be added to the CDE. These modules will either add new capabilities, or will substitute existing modules with new, higher fidelity, analysis capabilities. Examples are: high-fidelity structural mechanics including stiffness loop with aerodynamics, multi-level design of structural details, flutter analysis incorporating transonic corrections, lateral flight mechanics analysis, aircraft take-off aerodynamics in ground effect ... etc.

5.1 Acknowledgements

The study reported in this paper is carried out in the fifth framework of the European Commission's GROWTH programme; project MOB: *A Computational Design Engine Incorporating Multi-Disciplinary Design and Optimisation for Blended Wing Body Configuration*, contract number GRD1-1999-11162. The authors wish to thank the European Commission for partly funding the project and all partners who contributed to the functional modules which together form the CDE.

6 References

1. J.E. Green et al. *Air Travel - Greener by Design*. Society of British Aerospace Companies Ltd, London, 2002.
2. D.C. Montgomery. *Design and Analysis of Experiments*. Published by John Wiley and Sons, 1991.
3. W.J. Vankan. *A Spinware Based Computational Design Engine for Integrated Multi-Disciplinary Aircraft design*. AIAA-2002-5445, 9-th AIAA/ISSMO Symposium on Multi-disciplinary Analysis and Optimisation, Atlanta 2002.
4. G. La Rocca, L. Krakkers, M. van Tooren. *Development of an ICAD Generative Model for Blended Wing-Body Aircraft*. AIAA-2002-5447, 9-th AIAA/ISSMO Symposium on Multidisciplinary Analysis and Optimisation, Atlanta 2002.
5. D. Pearson. *MOB Structural Model Generation by PATRAN Session File* BAe-SYSTEMS, EC 5-th Framework Programme, Contract Number: GRD1-1999-11162. September 2001.
6. C. Healey. *Aerodynamic Pressure to Structural Loads Mapping using PALMS*. MOB/6/BAE/Report/1 , BAe-SYSTEMS.
7. ZONA Technology. *ZAERO Manuals, Version 4.3*. www.zonatech.com.
8. M. Stettner, R. Voss. *Aeroelastic, Flight Mechanics and Handling Qualities of the MOB BWB Configuration*. AIAA-2002-5449, 9-th AIAA/ISSMO Symposium on Multidisciplinary Analysis and Optimisation, Atlanta 2002.
9. P. Arendsen. *Final Report of the Garteur Action Group SM AG-21 on " Multi-Disciplinary Wing Optimisation "* NLR-TR-2001-557, 2001.
10. P. Arendsen, F. van Dalen, C. Bil, A. Rothwell. *ADAS Structures Module Evaluation Report* Presented at ISASTI 96, Jakarta, June 1996. Also issued as NLR-TP-95442.
11. P. Arendsen, F. van Dalen, C. Bil, and A. Rothwell. *Finite-Element based preliminary design procedures for wing structures* Presented at the 19-th ICAS conference, Los Angeles, September 1994. Also issued as NLR-TP-94450.
12. B.B. Prananta, I W. Tjatra, S.P. Spekreijse, J.C. Kok, J.J. Meijer. *Static Aeroelastic Simulation of Military Aircraft Configuration in Transonic Flow* International Forum on Aeroelasticity and Structural Dynamics, June 4-6 2001 in, Madrid, Spain. Also issued as NLR-TP-2001-346.
13. S.P. Spekreijse, J.C. Kok. *Semi-Automatic Domain Decomposition Based on Potential Theory* Presented at the 7th International Conference on Numerical Grid Generation in Computational Field Simulations, ed. B.K. Soni e.a., Whistler, Canada, 2000. Also issued as NLR-TP-2000-366.



14. S.P. Spekreijse, B.B. Prananta, J.C. Kok. *A Simple, Robust and Fast Algorithm to Compute Deformations of Multi-Block Structured Grids* Presented at the 8th International Conference on Numerical Grid Generation in Computational Field Simulations, ed. B.K. Soni e.a., Honolulu, Hawaii, 2002. Also issued as NLR-TP-2002-105.
15. J.C. Kok, S.P. Spekreijse. *Efficient and Accurate Implementation of the $k-\omega$ Turbulence Model in the NLR Multi-Block Navier-Stokes System*. Proceedings of the European Congress on Computational Methods in Applied Sciences and Engineering, ECCOMAS 2000, Barcelona, Spain. Also issued as NLR-TP-2000-144.
16. E. Torenbeek. *Synthesis of Subsonic Airplane Design*. Delft University Press, ISBN-90-247-2724-3, 1982.
17. D.M. Urie. *L-1011 Active Control, Design Philosophy and Experience*. AGARD-CP-260, May 1979.
18. P. Mangold. *Integration of Handling Quality Aspects Into the Aerodynamic Design of Unstable Fighters*. AGARD Symposium on Flying qualities, Quebec, October 1990.

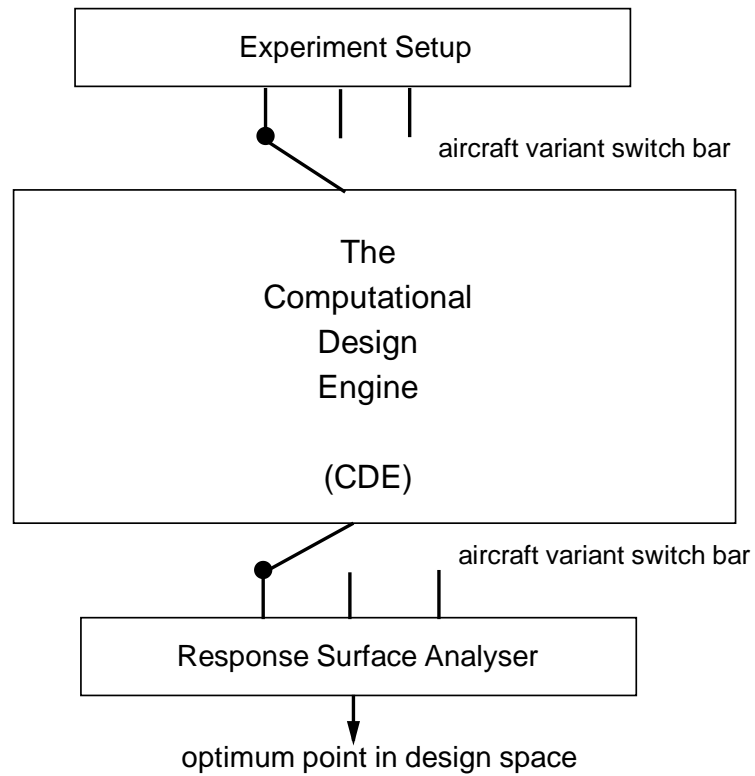


Fig. 1 The CDE, embedded in a response surface optimisation process, analyses the properties of aircraft design variants.

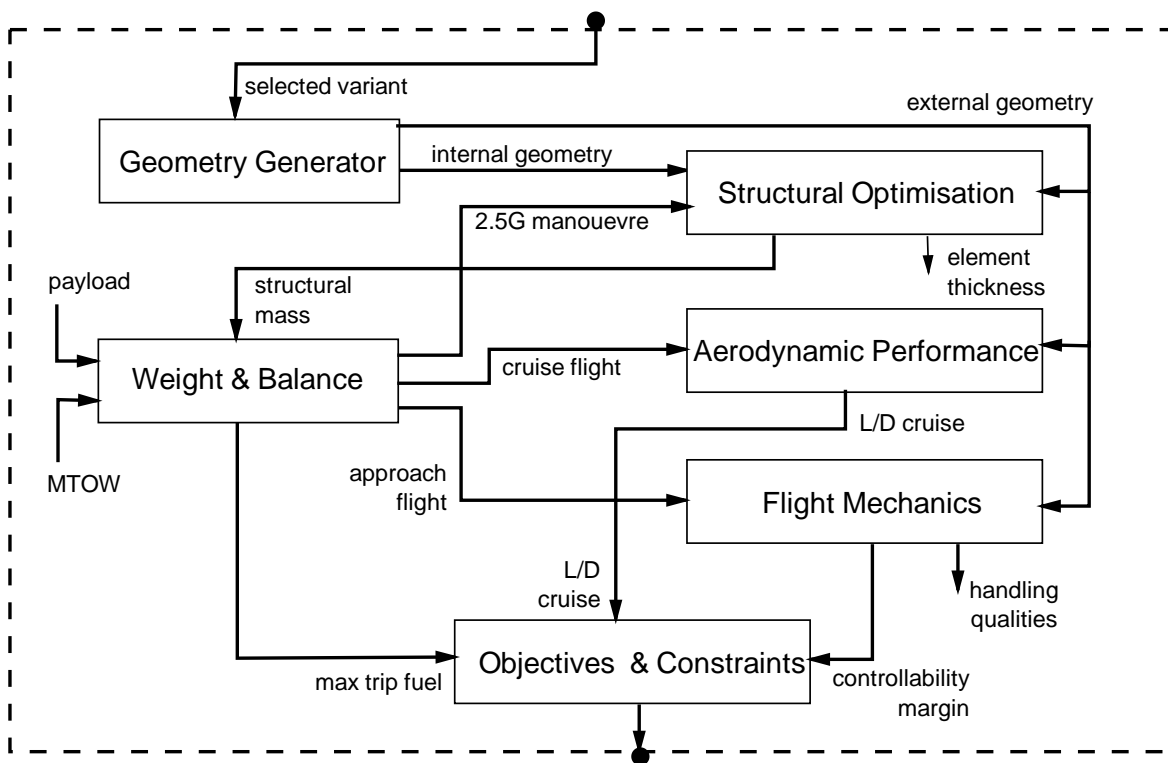


Fig. 2 The CDE features analysis modules from various disciplines.

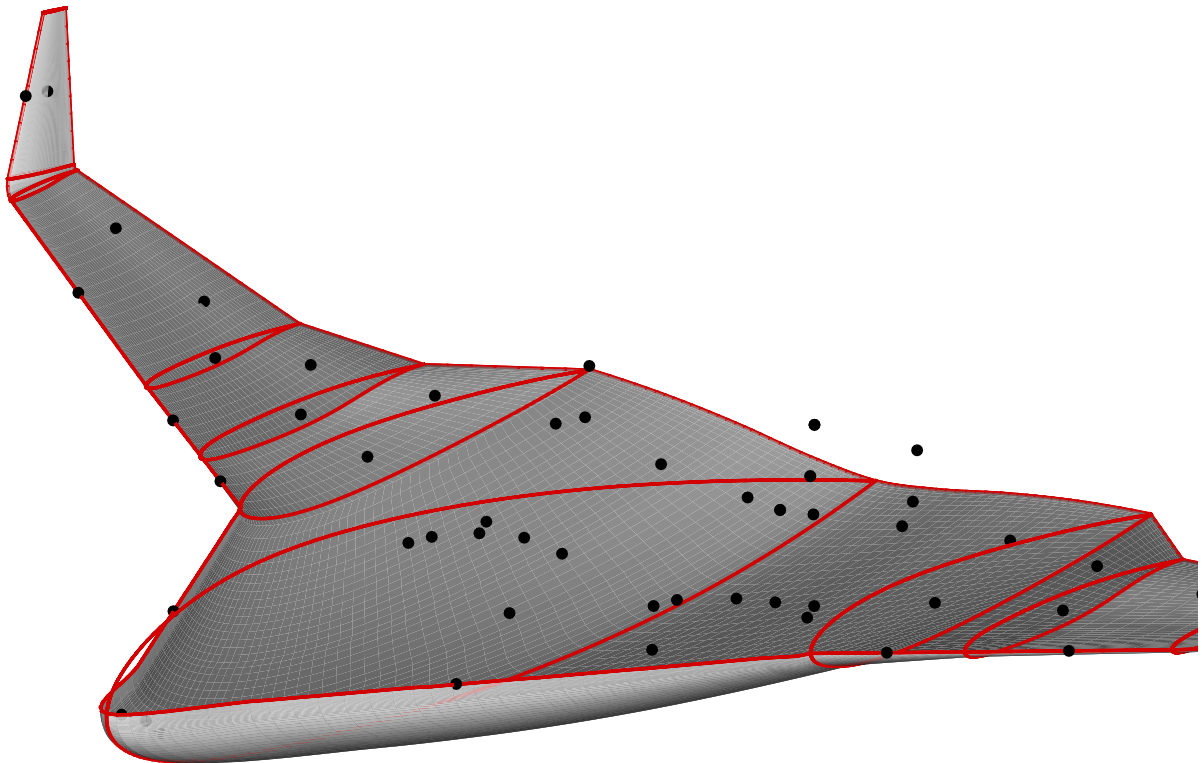


Fig. 3 The nonstructural items are represented as point masses connected to the aircraft structure (this includes the three fuselage mounted engines located outside the structure).

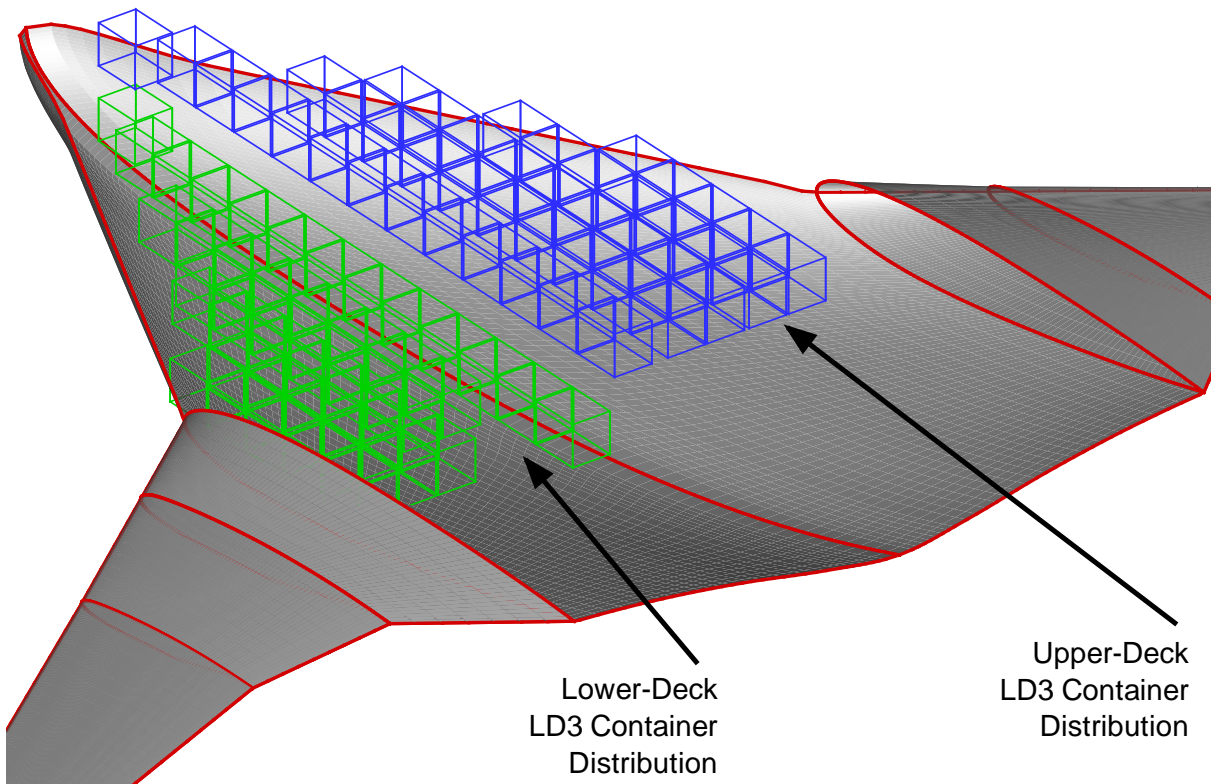


Fig. 4 The payload, 174 LD3 containers, are distributed over two decks in the cargo hold.

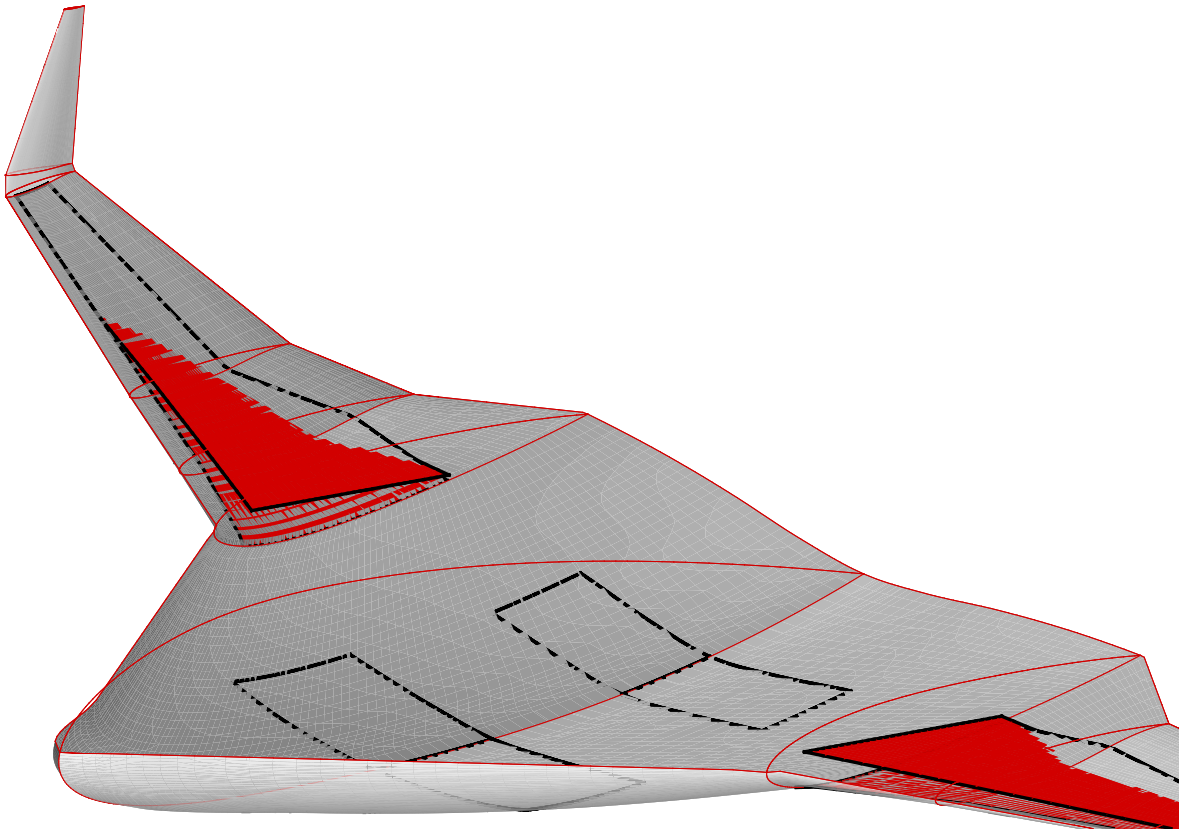


Fig. 5 Tank filling is under control of a fuel scheduler which distributes the fuel over the main wing tanks and two body trim tanks. The figure shows the situation at mid-cruise with maximum payload on board in which case the body trim tanks are not used.

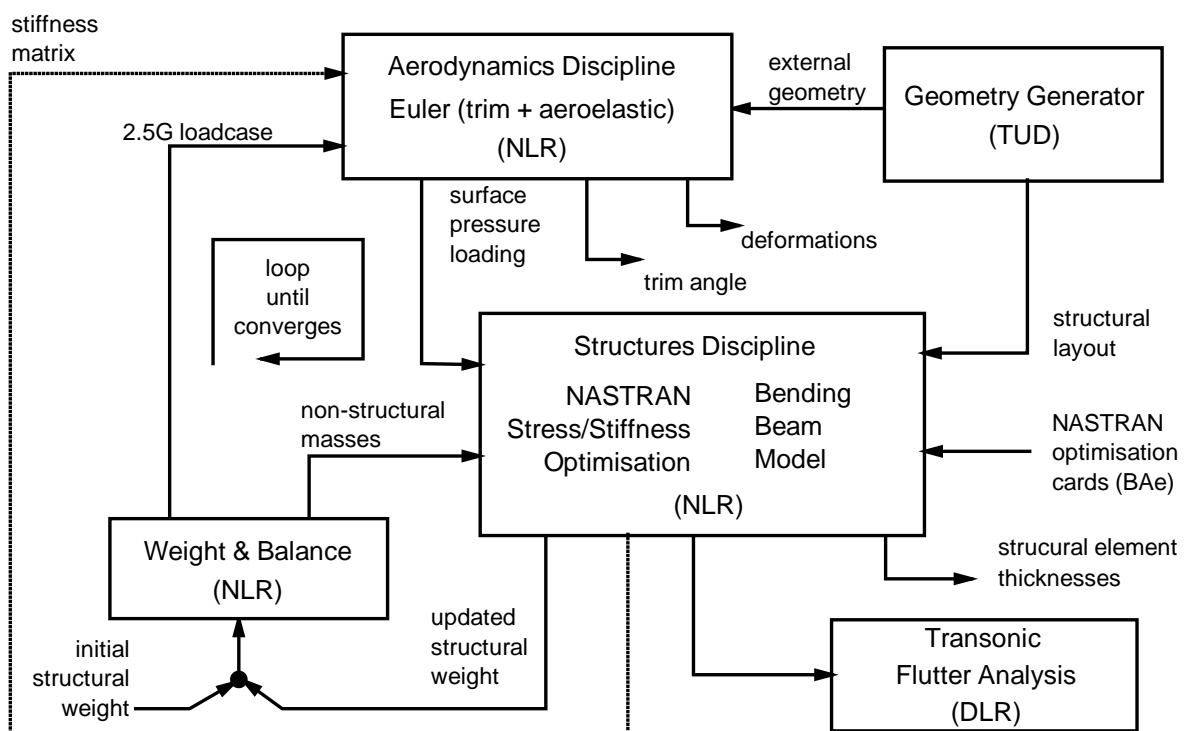


Fig. 6 The structural optimisation module comprising several disciplines in an iterative loop.

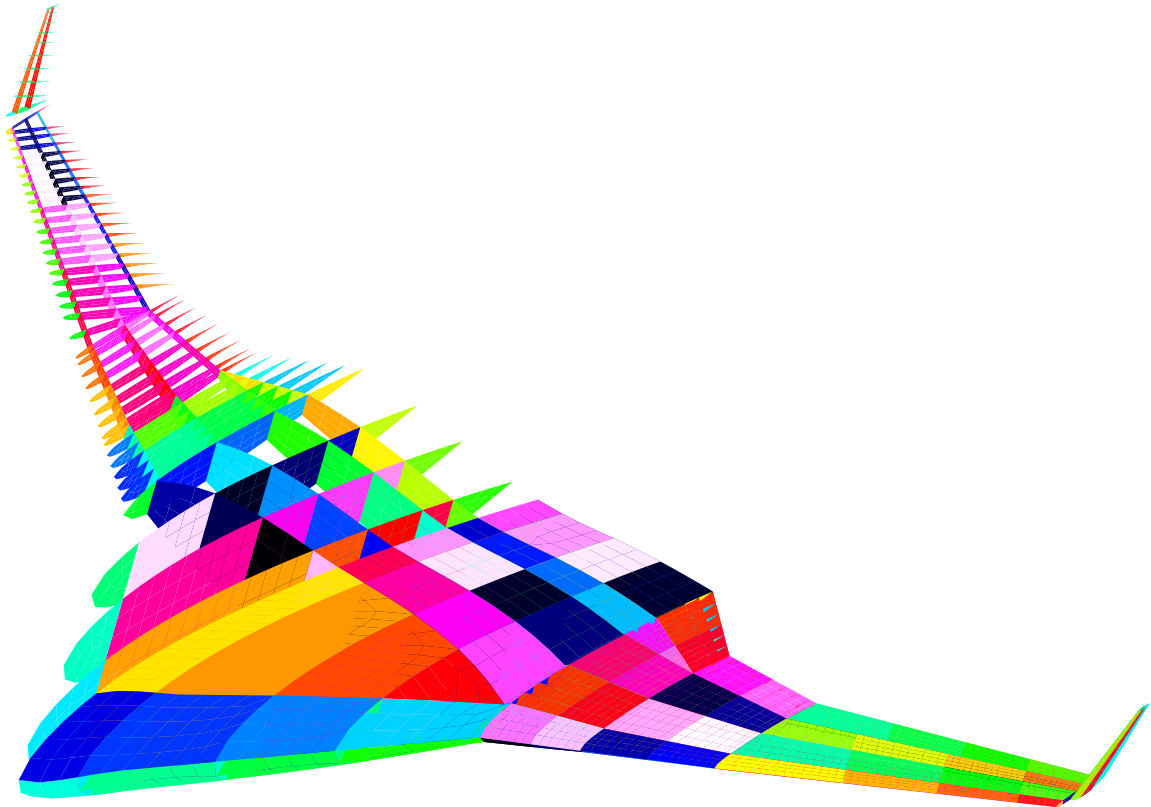


Fig. 7 The Blended Wing Body aircraft structure consists of spars, ribs, and skin panels. The structural elements are configured into 227 design variable areas which constitute the design parameters for the subsequent FEM optimisation.

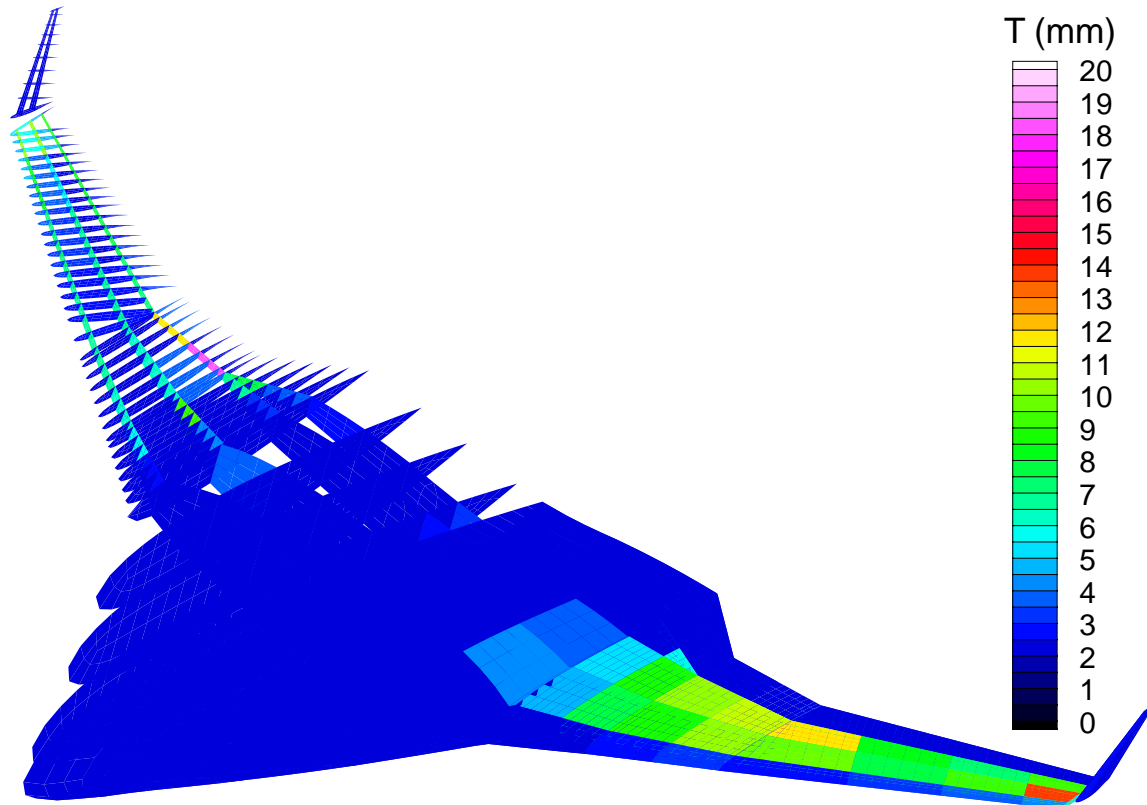


Fig. 8 FEM optimised element thicknesses for the Blended Wing Body aircraft. Optimisation objective is minimum weight. The thickness/stress/stiffness optimisation constraints are: $T > 2$ mm, $\sigma < 250$ N/mm² and $g > 0.03$ at $V=300$ m/s.

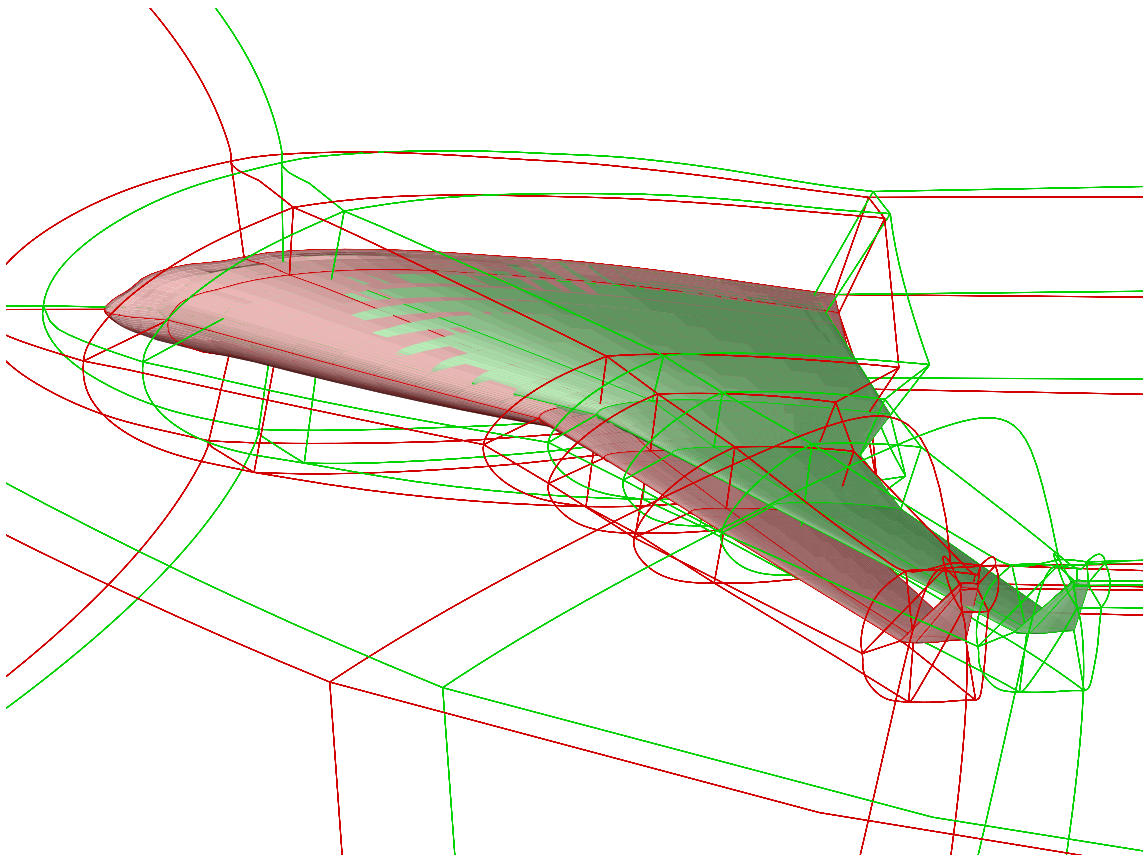


Fig. 9 Volume spline techniques are used to automatically map the reference aircraft multi-block topology to aircraft design variants.

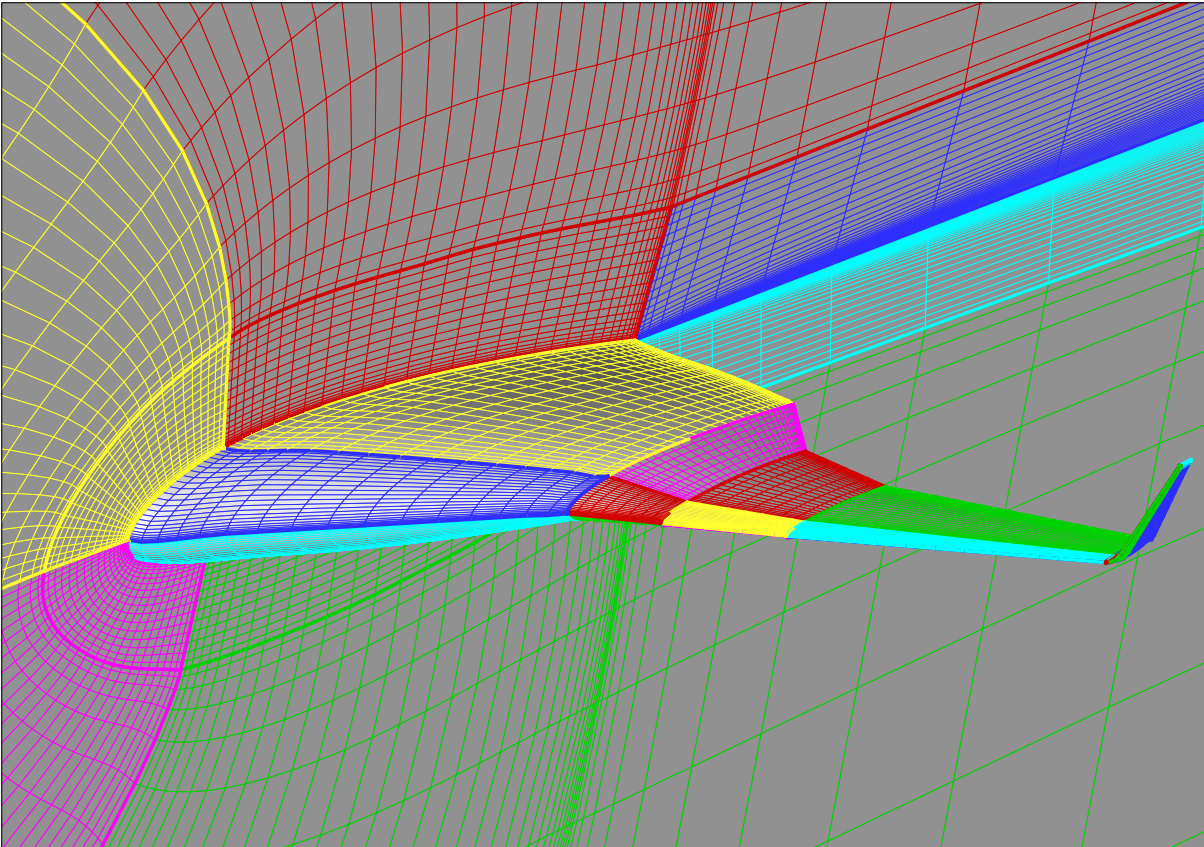


Fig. 10 A multi-block Navier-Stokes grid (552960 cells) is automatically produced for design variants using a parametric grid generator.

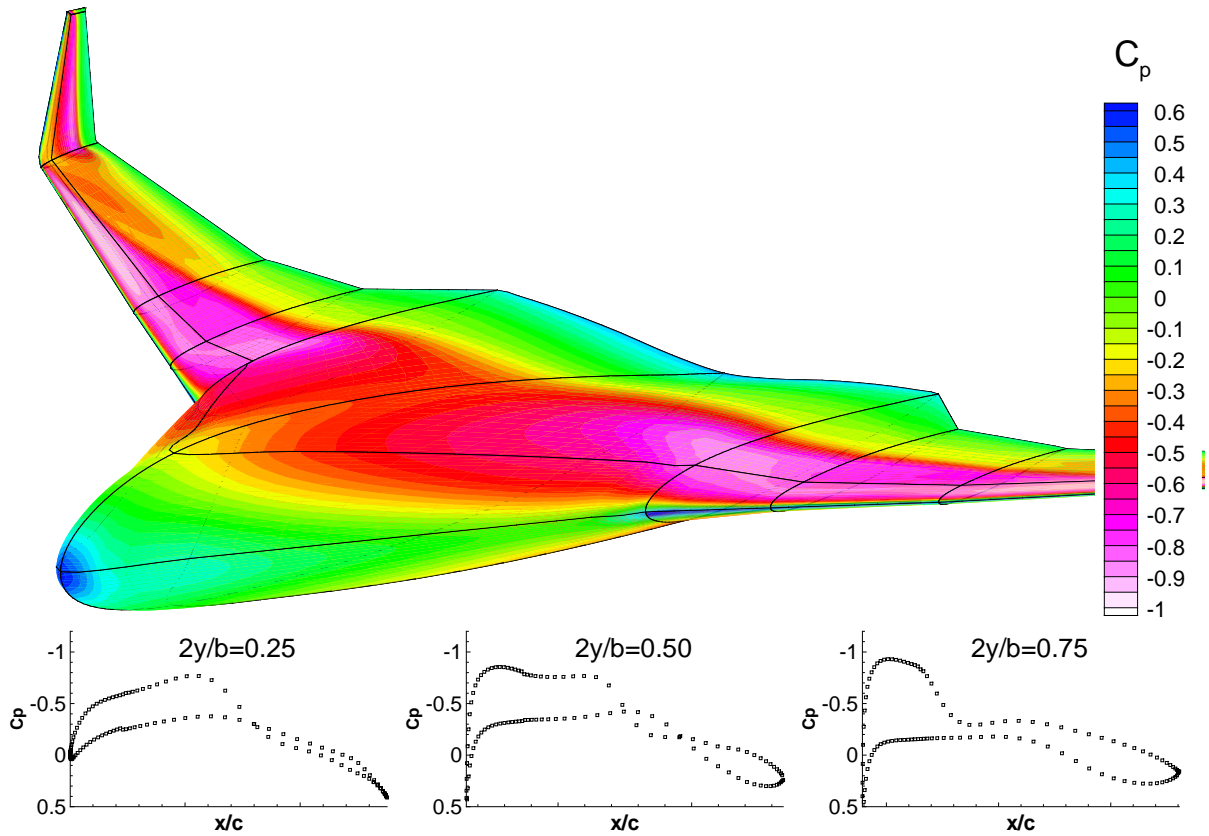


Fig. 11 Aerodynamic lift over drag performance is extracted from a Navier-Stokes flow solution at a Mach=0.85, $h=35000$ ft cruise flight condition.

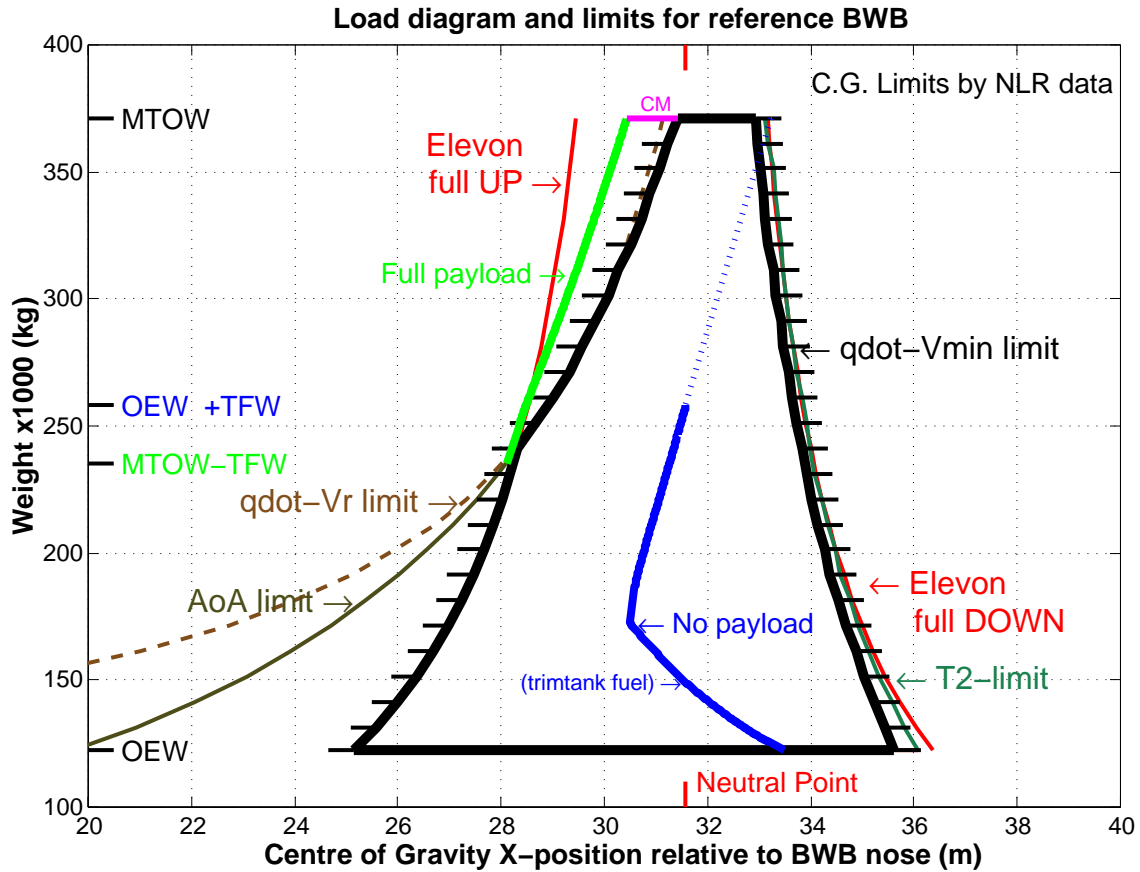


Fig. 12 The aircraft weight versus centre-of-gravity envelope. The flight mechanics discipline assesses the actual versus the tolerable envelope. The result is the Controllability Margin (CM), which is one of the driving constraints of the optimisation on the global level.

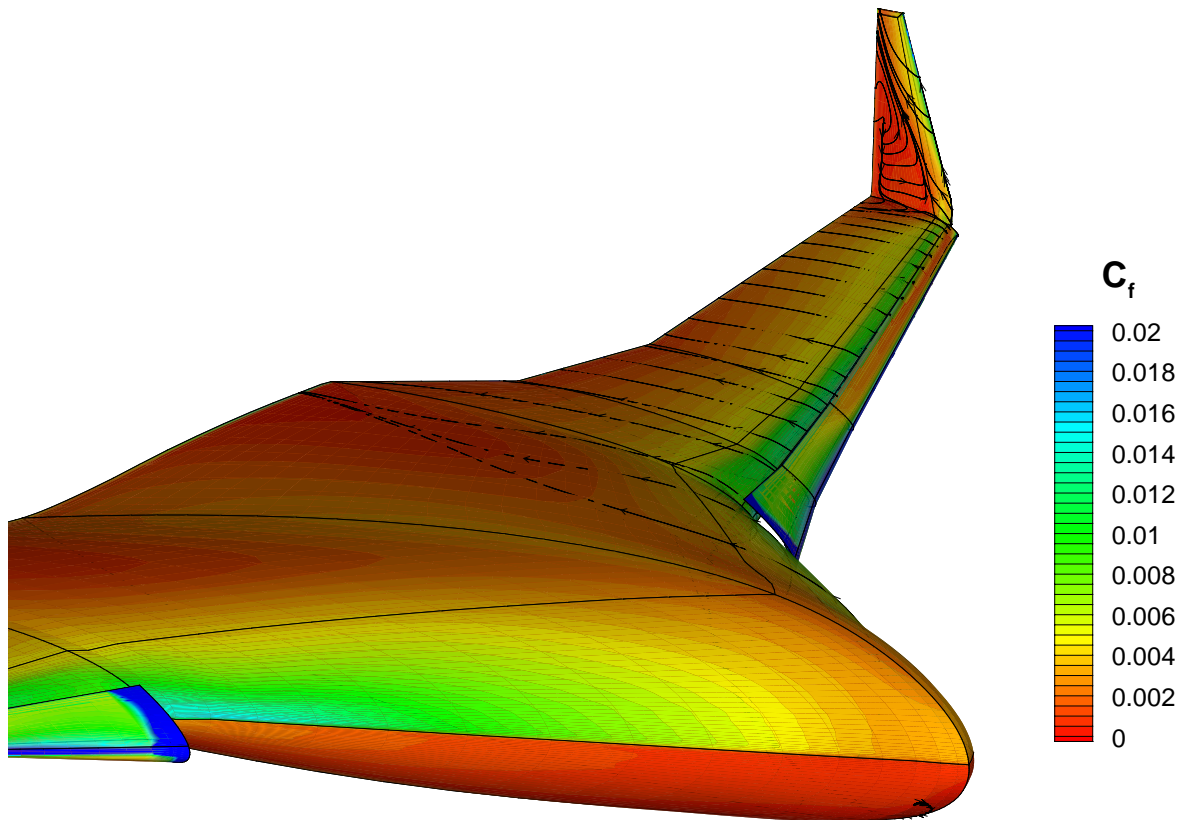


Fig. 13 A time accurate Navier-Stokes analysis provides maximum lift information during a dynamic stall for the BWB reference configuration with extended leading edge slats.

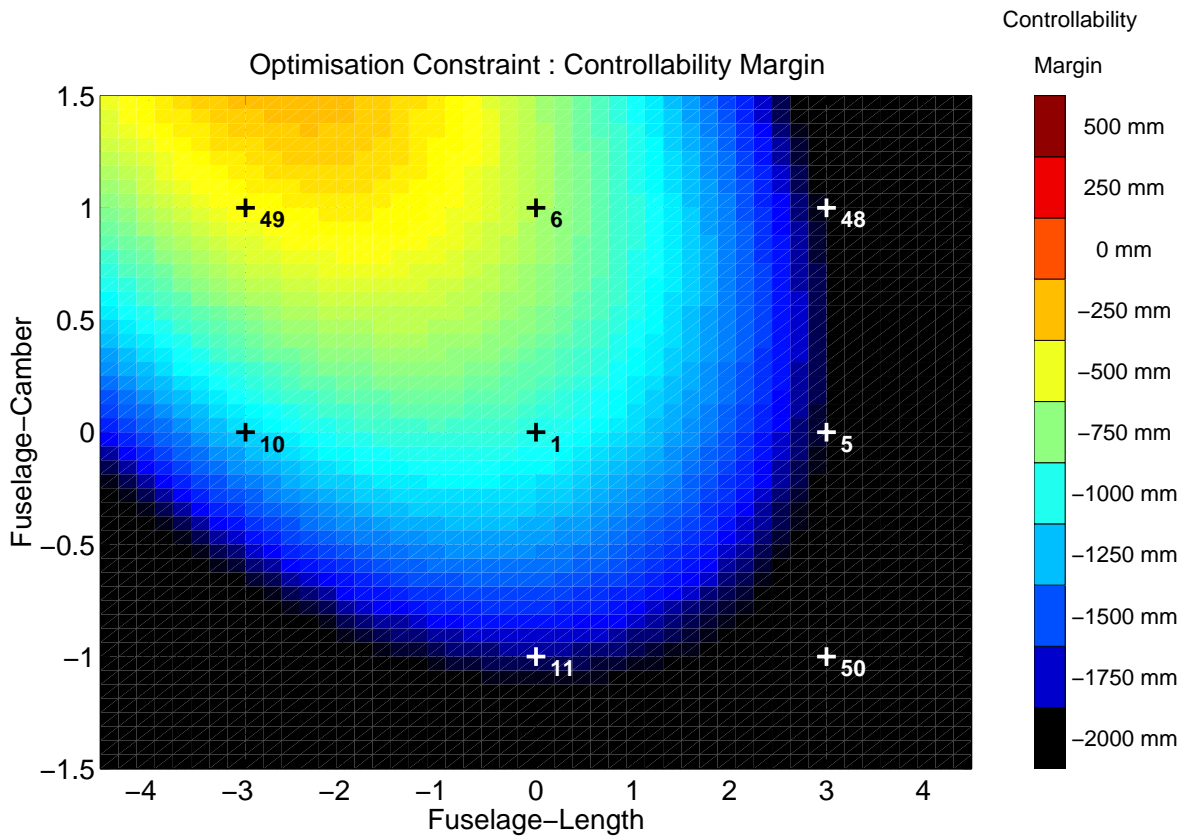


Fig. 14 Controllability Margin in the 2D Fuselage-Length offset ($\Delta\theta_4$) versus Fuselage-Camber offset ($\Delta\theta_5$) design space.

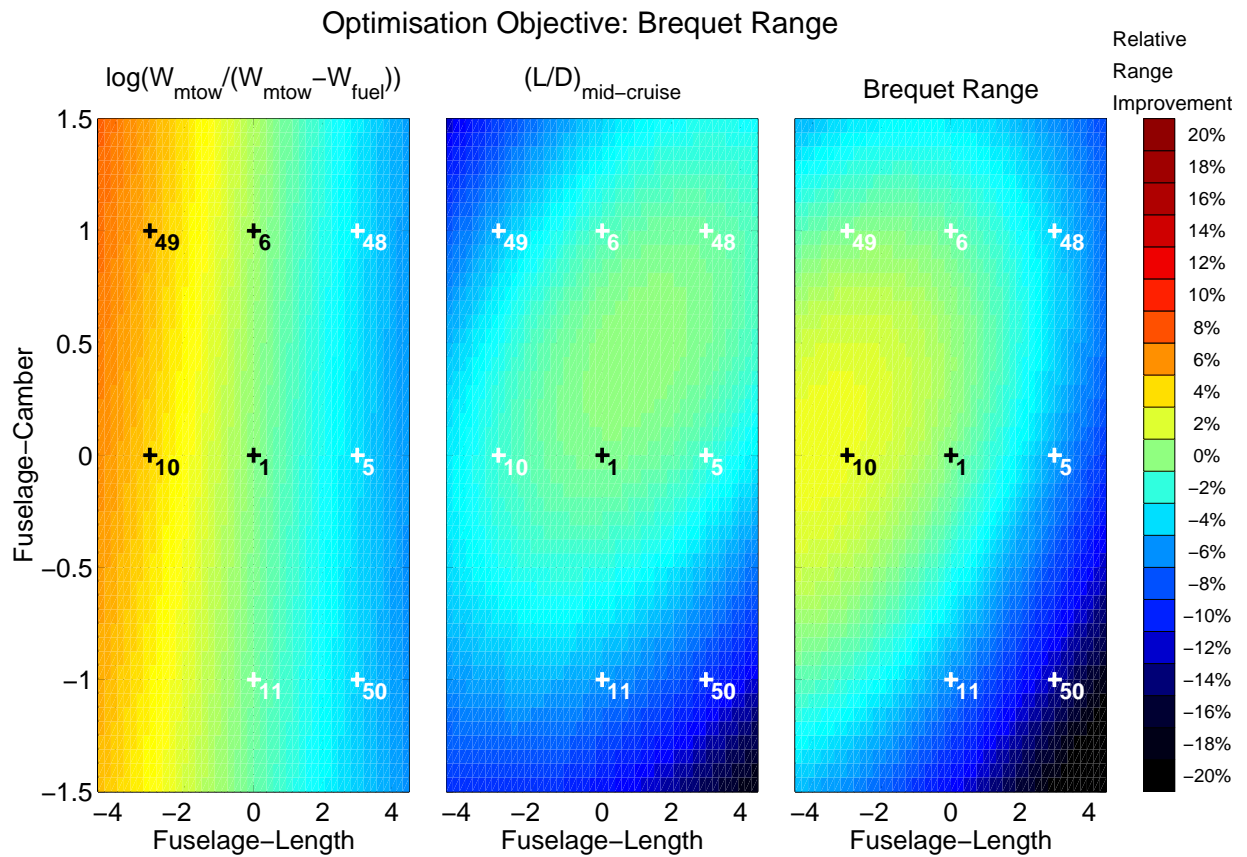


Fig. 15 Relative Breguet range improvement in the 2D Fuselage-Length offset ($\Delta\theta_4$) versus Fuselage-Camber offset ($\Delta\theta_5$) design space.

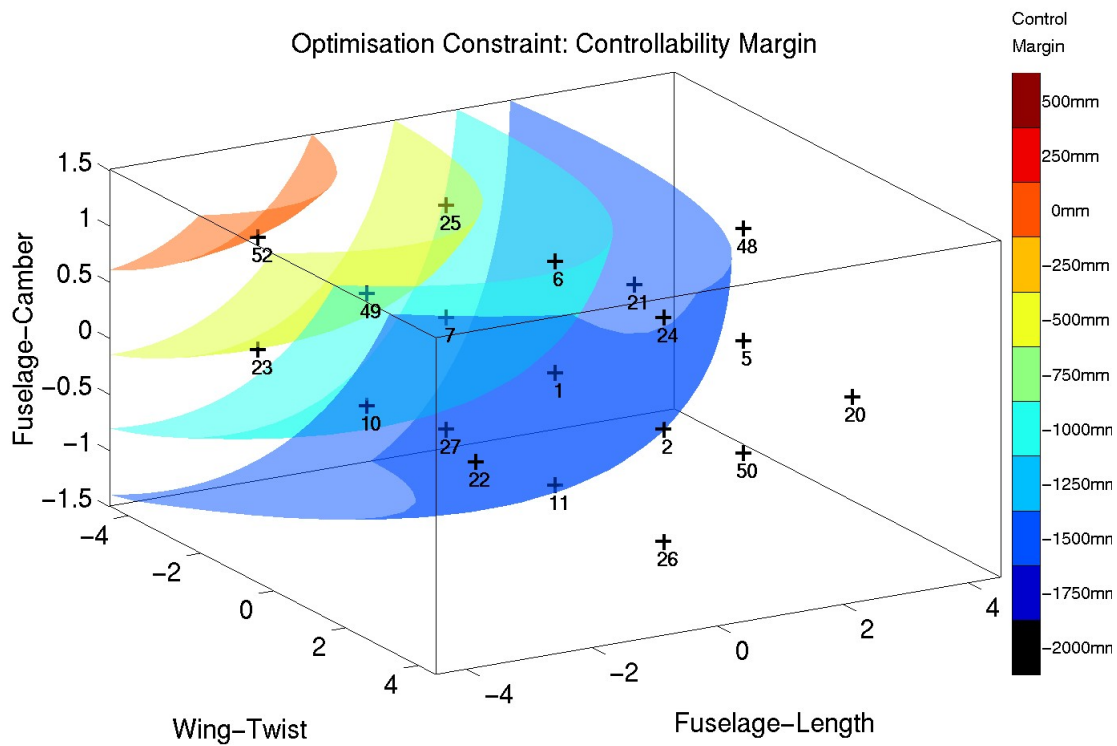


Fig. 16 Controllability Margin in the 3D Wing-Twist offset ($\Delta\theta_1$), Fuselage-Length offset ($\Delta\theta_4$) and Fuselage-Camber offset ($\Delta\theta_5$) design space.

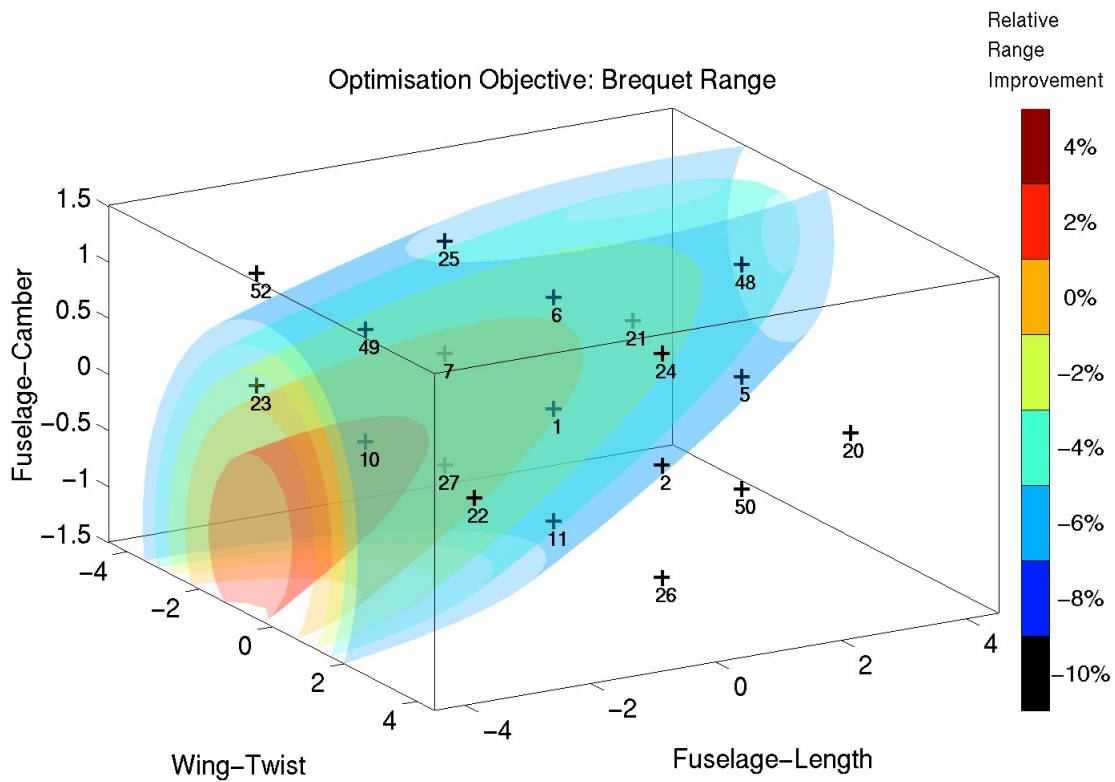


Fig. 17 Relative Breguet range improvement in the 3D Wing-Twist offset ($\Delta\theta_1$), Fuselage-Length offset ($\Delta\theta_4$) and Fuselage-Camber offset ($\Delta\theta_5$) design space.

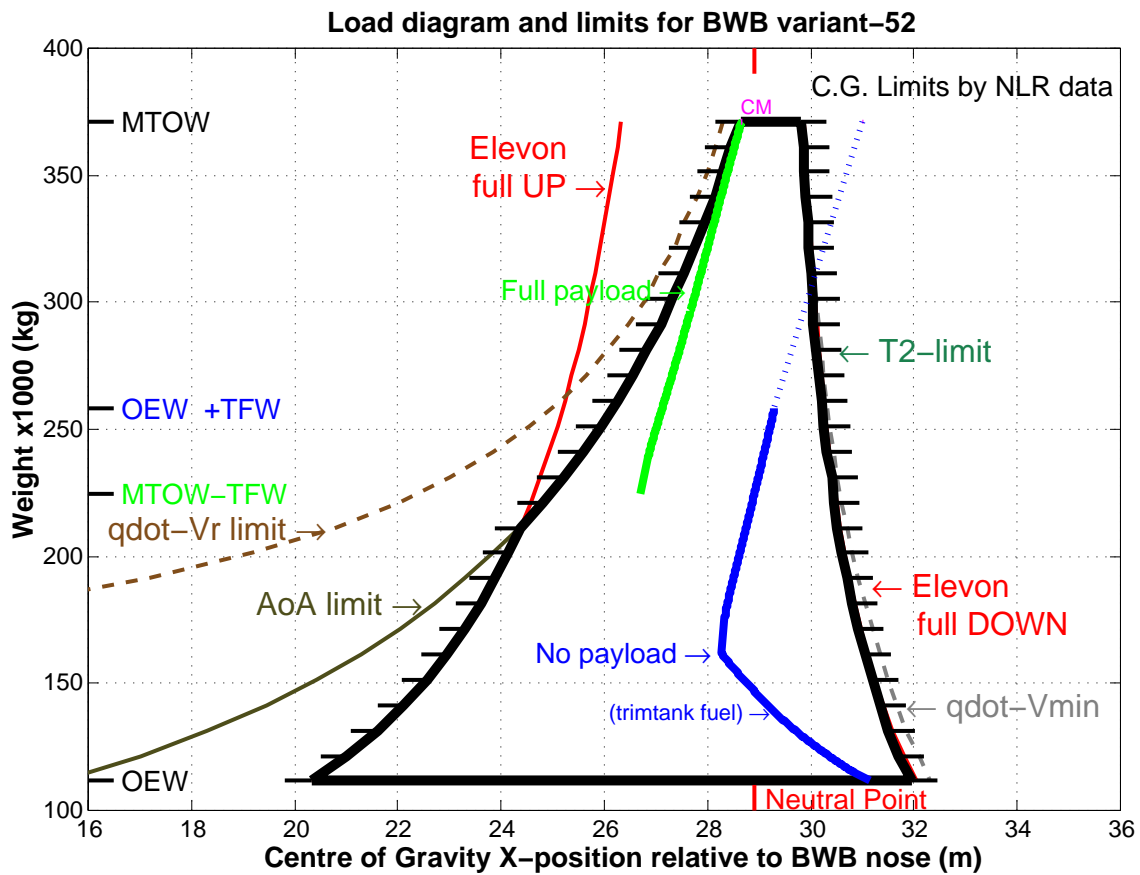


Fig. 18 The aircraft weight versus centre-of-gravity envelope of the -3° twisted wing ($\Delta\theta_1 = -3$), 3 m shortened fuselage ($\Delta\theta_4 = -3$) and 1 per cent aft-cambered fuselage ($\Delta\theta_5 = +1$) aircraft variant.